Light Absorption in Strongly Irradiated Long Range Polar Electron Transfer Systems

Yuri Dakhnovskii* and Vassiliy Lubchenko†

Department of Chemistry, Carnegie Mellon University, 4400 Fifth Avenue, Pittsburgh, Pennsylvania 15213

Rob D. Coalson

Department of Chemistry, University of Pittsburgh, Pittsburgh, Pennsylvania 15260

Light absorption of long range electron transfer (ET) complexes immersed in polar solvents is analyzed. At sufficiently high laser intensities absorption or emission of multiple photon quanta occurs. In addition, the equilibrium population of the two donor and acceptor electronic states is strongly perturbed from its field-off value. The combination of these two effects results in dramatic variations in the frequency dependence of the absorption cross section as a function of laser intensity. Certain bands in the absorption spectrum can be eliminated simply by changing the laser intensity. For commonly utilized mixed-valence transition metal ET complexes and polar solvents an applied electric field strength of $\approx 10^7$ V/cm should be sufficient to induce noticeable changes in the weak-field spectrum. [S0031-9007(96)01192-1]

Mixed-valence transition metal complexes are characterized by a large separation between donor and acceptor sites, and strong coupling to a polar medium [1]. The electron transfer (ET) and optical absorption properties of such systems are strongly influenced by these two features [2].

When a strong time-dependent field is applied along an electron transfer path, the probability to find the electron in the initial electronic state is dependent on the intensity and frequency of the field. For an isolated ET system (no interaction with solvent) the electron can even be trapped in the initially occupied site [3]. When this system is coupled to the solvent by strong electron-polar bath modes interactions, the tunneling rate exhibits a resonance structure [4a,5] as a function of the intensity parameter

$$a = \frac{\mu_0 E_0}{\hbar \omega}, \tag{1}$$

where μ_0 is the dipole moment difference between the initial and final electronic states, and E_0 and ω are the amplitude and frequency of the applied monochromatic electric field $E(t) = E_0 \cos(\omega t)$. Strong-field effects manifest themselves when $a > 1$. Because of the large separation, R, between donor and electron sites in the ET complex, the permanent dipole moment difference between donor and acceptor electronic states can be very large. This reduces the value of the electric field strengths needed to achieve $a > 1$. According to estimations made in Refs. [5,6], for $\mu_0 \simeq 70$ D ($R \simeq 15$ Å) the values of E_0 are about 10^6–10^7 V/cm, which is less than the field strengths expected to induce dielectric breakdown in the solvent. Moreover, the value of the breakdown field can be increased by utilizing a pulsed field [6]. In addition to the rate constants for forward and backward reactions, the equilibrium distribution between the donor and acceptor electronic states is also strongly dependent on the intensity and frequency of the field [5], with the same critical field conditions.

We are interested here in light absorption when a strong electric field is directed along the electron tunneling coordinate. A useful schematic of this process is shown in Fig. 1. The parabolas indicated by 1 and 2 represent the nuclear coordinate potential energy surfaces associated with donor and acceptor electronic states, respectively. In the weak-field limit the absorption process has been analyzed by Hush [2], who found a single Gaussian-like absorption band centered at the transition energy between donor and acceptor at the donor state equilibrium position (i.e., $\hbar \omega_{\max} = E_r + \epsilon$). This band can be considered as a Franck-Condon vibronic absorption spectrum with effective optical transition dipole moment μ_{12} given by [2]

$$\mu_{12} = \frac{\Delta}{\omega_{\max}} \mu_0, \tag{2}$$

where Δ is the electron tunneling matrix element [see Eq. (4) below]. The magnitude of Δ decreases rapidly as
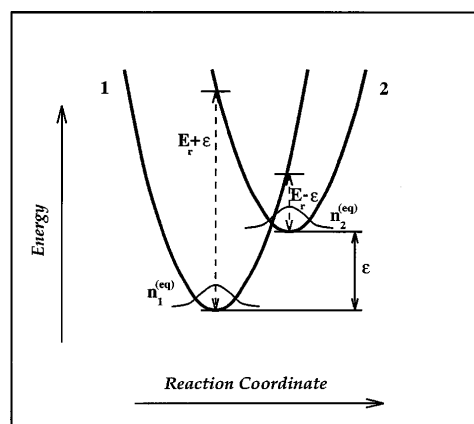

FIG. 1. Schematic depiction of the potential energy surfaces associated with electronic states 1 and 2 (donor and acceptor states, respectively) along the reaction coordinate. ϵ is the bias (the reaction heat), and E_r is the reorganization energy.

the intersite distance grows. For typical mixed valence systems $\hbar\Delta \approx 50$ cm^{-1}, while for typical polar solvents $\hbar\omega_{max} \approx 10\,000$ cm^{-1}. Thus $\Delta/\omega_{max} \approx 10^{-2}$ or smaller. This leads to the well-known fact that "mixed valence absorption bands are weak."

In this Letter, we analyze the strong-field absorption properties of such a system. It is thus useful to treat the electric field strength in a nonperturbative manner. Accordingly, we compute the average absorbed power, i.e., [7]

$$\frac{d\overline{E}}{dt} = \frac{1}{T} \int_0^T dt' \left\langle \frac{\partial \hat{H}}{\partial t'} \right\rangle \Bigg|_{T\to\infty}, \tag{3}$$

where $\hat{H}(t)$ is the time dependent Hamilton operator for the electron-solvent-applied electric field system. Specifically, we employ the field-driven spin-boson Hamiltonian utilized in recent work on electron transfer dynamics [4–6,8,9]

$$\hat{H}(t) = -\frac{1}{2}\hbar\Delta\hat{\sigma}_x - \frac{1}{2}\epsilon\hat{\sigma}_z + \frac{1}{2}\sum_k (p_k^2 + \omega_k^2 q_k^2)$$
$$+ \frac{1}{2}\hat{\sigma}_z \sum_k g_k q_k + \frac{1}{2}\mu_0 E(t)\hat{\sigma}_z. \tag{4}$$

Here ϵ is the bias (the reaction heat) between two equilibrium positions, $\hat{\sigma}_{x,z}$ are Pauli spin matrices, and ω_k and g_k are, respectively, the frequency and coupling constant of the kth bath oscillator described by coordinate q_k and momentum p_k. The electric state associated with the $|+\rangle$ eigenstate of $\hat{\sigma}_z$ (with eigenvalue $+1$) shall be designated as the donor electronic state (or state 1). The other electronic base state is then the acceptor state (or state 2).

An approximate generalized master equation, derived in Ref. [4] and by different methods in Refs. [8,9], is thought to give an accurate description of dynamics under $\hat{H}(t)$ in many cases. This kinetic equation (see, for example, Eq. (12) of Ref. [5]) is obtained by extension of the well-known noninteracting blip approximation (NIBA) associated with the standard spin-boson Hamiltonian [10,11] to include a time-dependent driving field [the last term in Eq. (4)]. In the absence of a driving field, the nonadiabatic electron transfer reactions exhibit overdamped, exponential relaxation to an asymptotic equilibrium state. It is well established that the NIBA describes such evolution adequately [10,12,13]. Recent work by Grifoni et al. [9a] indicates that for systems where the NIBA is accurate with no driving field, it should be at least as accurate when a high-frequency driving field is applied. This is precisely the case of interest here, since as already mentioned above, the ratio of Δ/ω is typically 10^{-2} or less. Therefore it is reasonable to adopt the NIBA generalized master equation as the starting point for our analysis.

In field-driven nonadabatic electron transfer systems, where the electronic tunneling matrix element is small, the environment is strongly coupled to the ET complex, and high laser frequencies (set by the solvent reorganization energy) are appropriate, analysis of the NIBA generalized

master equation shows that the electronic population dynamics evolves to good approximation in an exponential fashion [5]:

$$n_1(t) = n_1^{(eq)} + n_2^{(eq)}\exp[-(\Gamma_1 + \Gamma_2)t],$$
$$n_2(t) = n_2^{(eq)} - n_2^{(eq)}\exp[-(\Gamma_1 + \Gamma_2)t], \tag{5}$$

with

$$n_1^{(eq)} = \frac{\Gamma_2}{\Gamma_1 + \Gamma_2},$$
$$n_2^{(eq)} = \frac{\Gamma_1}{\Gamma_1 + \Gamma_2}, \tag{6}$$

where Γ_1 and Γ_2 are the forward and backward rate constants which are in general strongly field dependent. In particular, when only classical (low frequency) oscillator modes associated with the solvent dynamics are taken into account, these constants take the form [5]

$$\Gamma_{1,2} = \frac{\hbar\Delta^2}{4}\left(\frac{\pi}{E_r k_B T}\right)^{1/2} \sum_{m=-\infty}^{\infty} J_m^2(a)$$
$$\times \exp\left(-\frac{(E_r \pm \epsilon - m\hbar\omega)^2}{4E_r k_B T}\right). \tag{7}$$

[$+$, $-$ choices on the right-hand side go with subscripts 1, 2, respectively, on the left-hand side.] The structure of this expression for the rate constants allows the following interpretation of relaxation dynamics in a strong $c\omega$ laser field. The rate constant is a sum of many contributions each of which is proportional to the nonadiabatic transition rate for a system in which the bias between donor and acceptor sites has been shifted by m photon quanta. The probability of making a transition through the mth such "channel" is also proportional to $J_m^2(a)$, where J_m is the mth order Bessel function. One can vary the contribution of each channel dramatically by changing the laser intensity, i.e., the parameter a [see Eq. (1)] [4a,5].

The rate constant formula (7) combined with the interpretation given in the previous paragraph suggests that the contribution of the mth channel to the ET rate at laser frequency ω is associated with multiphoton absorption or emission of m photon quanta of magnitude $\hbar\omega$. Indeed, by analyzing the full NIBA master equation, it is possible to evaluate Eq. (3) and thus derive the following formula for the absorption or emission rate from the donor and acceptor electronic states [14,15]:

$$\frac{d\overline{E(a,\omega)}}{dt} = n_1^{(eq)}\frac{\partial U_1}{\partial t} + n_2^{(eq)}\frac{\partial U_2}{\partial t}. \tag{8}$$

Here $n_{1,2}^{(eq)}$ are the equilibrium populations of electronic states 1 and 2 (donor and acceptor), which are themselves field dependent. These values prescribe the size of the "reservoir" of populations in the donor and acceptor states after steady state has been obtained. The quantities

$\partial U_{1,2}/\partial t$ are the rates of energy absorption per molecule in states 1 and 2, respectively, and are given by

$$\frac{\partial U_{1,2}}{\partial t} = \frac{\hbar \Delta^2}{4} \left(\frac{\pi}{E_r k_B T}\right)^{1/2} \sum_{m=1}^{\infty} m\hbar\omega J_m^2(a)$$

$$\times \left[\exp\left(-\frac{(E_r \pm \epsilon - m\hbar\omega)^2}{4E_r k_B T}\right) \right.$$

$$\left. - \exp\left(-\frac{(E_r \pm \epsilon + m\hbar\omega)^2}{4E_r k_B T}\right)\right].$$

$$(9)$$

The structure of Eq. (9) is simple. The $m = 0$ contribution, which corresponds to thermal electron transfer without optical absorption, is absent. The surviving terms correspond to absorption and emission of m photons (the first and second terms, respectively, in the summand). The probability of an m-photon absorption or emission event *is exactly as anticipated from the ET rate constant formula (7)*.

We define the absorption cross section as the ratio of the average absorbed power to the average incident power [8]. The average absorbed power is given in Eqs. (8) and (9). The average incident power is proportional to the Poynting vector, whose cycle-averaged magnitude for a monochromatic radiation field is $cE_0^2/8\pi$. Thus,

$$k_{\mathrm{abs}} = \frac{8\pi}{cE_0^2} \frac{d\overline{E(a,\omega)}}{dt}. \qquad (10)$$

We wish to study the dependence of the absorption cross section on laser frequency. In general, this cross section also depends on electric field strength, so that the variation of the latter quantity with laser frequency must also be specified. Thus, we illustrate expression (10) for two different scanning procedures.

First we keep the dimensionless intensity parameter a constant as the laser frequency is changed (which requires that the field strength be changed proportionately). The resultant frequency spectrum is shown in Fig. 2 at different a for the barrierless reaction with $\epsilon = E_r = 1$ eV and $k_B T = 200$ cm^{-1} (room temperature). (All spectra in this and subsequent figures are normalized to have unit area.) When the intensity is low, i.e., $a = 0.2$, there is only one absorption peak, due to 1-photon absorption from the initial state. This band agrees in shape and integrated intensity with the well-known prediction of Hush [2] (c.f. also the discussion in Ref. [14]). At moderate intensities, $a = 1.0$, a second band appears, corresponding to 2-photon absorption from the initial state. At higher laser intensities, the amplitude of the main absorption peak becomes lower while the amplitudes of the 2-photon and 3-photon absorption bands become higher. At $a = 2.4$, the first zero of J_0, the main absorption band disappears completely, because the equilibrium population $n_1^{(\mathrm{eq})}$ in the initial electronic state vanishes, even though the intrinsic probability of a 1-photon absorption from a molecule prepared in this state is nonzero. At $a = 3.8$
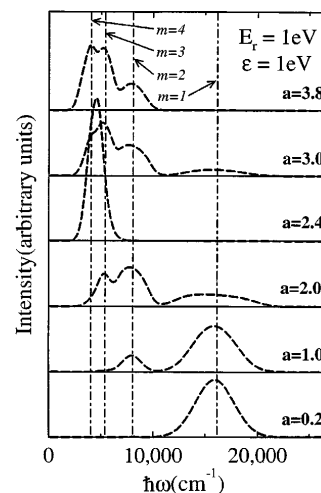

FIG. 2. The absorption spectrum at different intensities a for the activationless reaction $E_r = \epsilon$. The spectrum is calculated at constant a. The vertical dotted lines indicate the expected peak positions of the 1-, 2-, 3-, and 4-photon absorption bands.

(the first zero of J_1), the main band disappears again, because the probability of 1-photon absorption is zero even though the equilibrium population $n_1^{(\mathrm{eq})}$ is not zero at this intensity.

In Fig. 3, the absorption spectrum for the symmetric complex ($\epsilon = 0$) is presented. In this case $n_1^{(\mathrm{eq})} = n_2^{(\mathrm{eq})} = 0.5$ for all frequencies; hence the absorption spectrum is not affected by field dependence of the population distribution. At low laser intensities there is 1-photon absorption only. At $a = 1$ a shoulder from the 2-photon absorption band arises. When $a = 2.4$, the second peak is larger than the 1-photon band peak. At a higher intensity, $a = 3$ (not shown), three bands contribute to the spectrum. The 1-photon absorption band is completely suppressed at $a = 3.8$ [$J_1(3.8) = 0$].

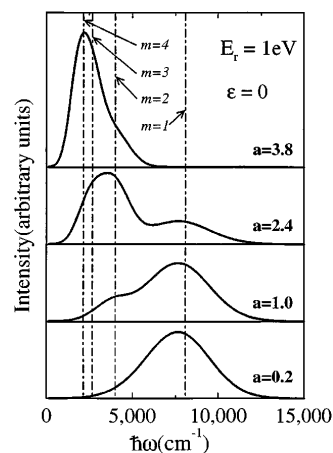Experimentally it may be more convenient to measure the spectrum at constant laser intensity (i.e., constant E_0)

FIG. 3. The absorption spectrum at different intensities a for the symmetric reaction $\epsilon = 0$. The spectrum is calculated at constant a.

rather than at constant a. In Fig. 4 the absorption spectrum is shown at different values of the laser intensity. We choose E_0 in order to make the parameter a have the indicated value at the center of the 1-photon absorption band ($\hbar\omega_{max} = E_r + \epsilon = 2$ eV). The parameters are the same as in Fig. 2 ($E_r = \epsilon$). At low intensity ($a = 0.2$) the 1-photon band dominates. The 2-photon subharmonic is weak but detectable. At higher intensities, the 2-photon absorption band is strong enough to be easily discerned. In addition, some fine structure arises in the low frequency part of the spectrum, which might be misinterpreted if ascribed to resolved transitions between specific vibrational levels. When $a = 2.4$ (a zero of J_0), there is no population in the initial state. Consequently, there is no absorption at the 1-photon resonance frequency, while an unusual band appears at a higher frequency. This is due to complicated interplay between two factors: $n_1^{(eq)}$ and $\partial U_1/\partial t$ in Eq. (8). At $a = 3.8$, absorption at the weak-field 1-photon absorption resonance frequency is suppressed again, this time due to vanishing of the absorption coefficient $\partial U_1/\partial t$. The peak structure is again complicated for the reasons just noted.

In conclusion, we have studied strong field light absorption in a long-range electron transfer system such as a mixed valence transition metal complex coupled to a strongly dissipative environment. When the distance between electron donor and acceptor centers is large, strong-field effects can be achieved with electric fields that are not unrealistically large. Absorption of one or more quanta of light can occur from both donor and acceptor electronic states. The absorption strength associated with either configuration is scaled by the steady-state electronic population in that configuration. The pronounced intensity dependence of both the intrinsic multiphoton transition probabilities and the steady-state
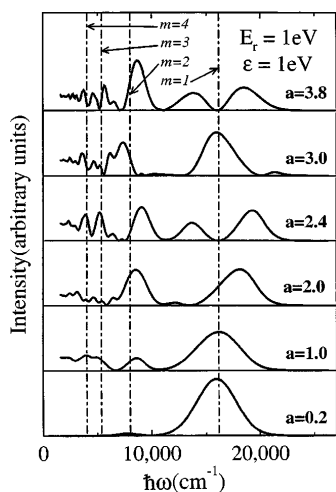
equilibrium populations enables suppression and enhancement of various bands in the absorption spectrum simply by tuning the laser intensity.

The calculated absorption spectrum has been obtained assuming that all reactive systems are aligned along the field direction. However, even for nonoriented samples, the effect described above should be qualitatively observable. For a barrierless reaction, detection of a band at half the frequency of the main (weak-field) absorption band would demonstrate the existence of the effect.

*Current address: Department of Chemistry, University of Pittsburgh, Pittsburgh, PA 15260.
†Current address: Department of Chemistry, University of Illinois, Urbana, IL 61801.

[1] H. Taube, in *Tunneling in Biological Systems,* edited by B. Chance *et al.* (Academic Press, New York, 1979), p. 173.
[2] N. S. Hush, Electrochim. Acta **13**, 1005 (1968); Prog. Inorg. Chem. **8**, 391 (1967).
[3] F. Grossmann, T. Dittrich, P. Jung, and P. Hänggi, Phys. Rev. Lett. **67**, 516 (1991).
[4] (a) Yu. Dakhnovskii, J. Chem. Phys. **100**, 6492 (1994); (b) Phys. Rev. B **49**, 4649 (1994); (c) Ann. Phys. (N.Y.) **230**, 145 (1994).
[5] Yu. Dakhnovskii and R. D. Coalson, J. Chem. Phys. **103**, 2908 (1995).
[6] D. G. Evans, R. D. Coalson, H. Kim, and Yu. Dakhnovskii, Phys. Rev. Lett. **75**, 3649 (1995).
[7] L. D. Landau and E. M. Lifshitz, *Electrodynamics of Continuous Media* (Pergamon Press, New York, 1960).
[8] I. A. Goychuk, E. G. Petrov, and V. May, Phys. Rev. E **52**, 2392 (1995).
[9] (a) M. Grifoni, M. Sassetti, P. Hänggi, and U. Weiss, Phys. Rev. E **52**, 3596 (1995); (b) M. Grifoni, M. Sassetti, and U. Weiss, Phys. Rev. E **53**, R2033 (1996).
[10] A. J. Leggett *et al.,* Rev. Mod. Phys. **59**, 1 (1987).
[11] C. Aslangul, N. Pottier, and D. Saint-James, J. Phys. (Paris) **47**, 1657 (1986).
[12] A. Garg, J. N. Onuchic, and V. Ambegaokar, J. Chem. Phys. **83**, 4491 (1985); M. Sparpaglione and S. Mukamel, J. Chem. Phys. **88**, 3263 (1988).
[13] D. G. Evans, R. D. Coalson, and A. Nitzan, J. Chem. Phys. **101**, 436 (1994); D. G. Evans and R. D. Coalson, J. Chem. Phys. **102**, 5658 (1995).
[14] Yu. Dakhnovskii, V. Lubchenko, and R. D. Coalson, J. Chem. Phys. (to be published).
[15] This analysis includes the characterization of small oscillations around the steady-state value of the electronic populations predicted by Eqs. (5)–(7). A related analysis in a different context has been provided by Grifoni *et al.* in Ref. [10a]. Full details of our calculations are contained in Ref. [14].

FIG. 4. The absorption spectrum at different laser intensities, i.e., at fixed E_0^2. The values of the parameter a are taken at the frequency of the main weak-field absorption peak, $\hbar\omega_{max} = E_r + \epsilon$.